Nonrotational states in isotonic chains of heavy nuclei

G. G. Adamian and L. A. Malov*
Joint Institute for Nuclear Research, 141980 Dubna, Russia

N. V. Antonenko
Joint Institute for Nuclear Research, 141980 Dubna, Russia
and Mathematical Physics Department, Tomsk Polytechnic University, 634050 Tomsk, Russia

R. V. Jolos
Joint Institute for Nuclear Research, 141980 Dubna, Russia
and Dubna State University, 141980 Dubna, Russia

(Received 10 November 2017; revised manuscript received 15 January 2018; published 6 March 2018)

The ground-state deformations of heavy nuclei are explored with the microscopic-macroscopic approach using the single-particle Woods-Saxon potential of the quasiparticle-phonon model. The calculations of the energies of low-lying nonrotational states take into account the residual pairing and phonon-quasiparticle interactions. The spectra of these states are presented for the $N = 147$–161 isotones. The sensitivity of the calculated results to the parameters of the model is studied. A rather good description of the available experimental data is demonstrated.

DOI: 10.1103/PhysRevC.97.034308

I. INTRODUCTION

Recent intensive experimental studies of superheavy nuclei [1–7] resulted in the discovery of new nuclei and obtained information on single-particle states and nuclear deformations. The systematic calculations of single-particle spectra of the heaviest nuclei have been performed in Refs. [8–11]. However, the interaction of quasiparticles with phonons, which is determined by the mean-field fluctuations, has not be taken into account there. As shown within the relativistic quasiparticle-vibration model [12–14], the inclusion of collective vibrations and their coupling to quasiparticles improves description of the experimental spectra.

Besides the self-consistent approach mentioned, the residual interaction is also considered in the quasiparticle-phonon model (QPM) [15–19], which allows us to describe well the structure of deformed rare-earth-metal nuclei and actinides with $A > 228$ [20–29]. In this model, the nuclide chart is divided into a few regions around some Z and A in which the parameters of the mean field and the residual interaction are fixed. This corresponds to the choice of some average deformation and other model parameters for all the nuclei of each region. The calculations of the equilibrium deformations of nuclei [10,11,30] mainly confirm the validity of such a rough approximation for nuclei far from the magic or semimagic ones. However, it has been experimentally found [31] that the deformations of some nuclei even with close values of Z or A can differ. In these cases, one should take into account the difference of mean fields of these nuclei because some low-lying states are very sensitive to the deformation and the calculation with a fixed deformation would lead to a large error, within 0.5–1 MeV, in the determination of the state energy. Therefore, to carry out the correct calculations for each nucleus, its equilibrium deformation has to be defined. This is especially important when the calculations are performed for poorly studied nuclei. It is also important for prediction of the properties of nuclei that are as of yet uninvestigated. The calculations should have minimum uncertainties when they are performed for superheavy nuclei or for nuclei located far from the β-stability line, neutron-deficient or neutron-rich nuclei, and isomeric states. Indeed, the experimental study of these nuclei is time-consuming and requires reliable predictions.

The microscopic methods, which are used to study the structure of heaviest nuclei, are the self-consistent approaches (nonrelativistic and relativistic) [32–46] based on some parametrization of energy-density functional and the microscopic-macroscopic methods [10,11,30,47–52] in which the parameters are introduced to write down the single-particle potential and to find the macroscopic part of potential energy.

In the present work, the excitation energy spectra of transcurie nuclei are calculated with the QPM [16,53–56] for equilibrium deformations. Our intention is to use the QPM for describing the ground states and low-lying nonrotational states in heavy nuclei. As the first step, we incorporate the QPM Woods-Saxon potential into the microscopic-macroscopic approach. So, the ground-state deformations are not the parameters of the QPM anymore, as before. As demonstrated, this development of the QPM is reliable and can be the basis for further work related to the calculation of the total binding energies, charge, and mass radii. In Sec. II, the main ingredients of the QPM are presented. The equilibrium deformations are defined with the microscopic-macroscopic approach in Sec. III. Because the experimental information for the most of heavy

*malov@theor.jinr.ru

nuclei investigated is still rather scarce or nonexistent, there are difficulties with choosing the parameters of the model. Therefore, in Sec. IV we analyze the dependence of the results obtained on the parameters used to choose their optimal values. The spectra of low-lying nonrotational states in a few isotonic chains are discussed in Sec. V.

II. MODEL

The QPM Hamiltonian is as follows [15,16]:

$$H = H_{sp} + H_{\rm pair} + H_M + H_{SM}. \quad (1)$$

The mean-field potential V_{sp} in H_{sp} contains the central potential V_{WS} in the Woods-Saxon (WS) form for neutrons and protons, the spin-orbit part $V_{so}(\mathbf{r})$, and the Coulomb field $V_C(\mathbf{r})$ for protons:

$$V_{sp}(\mathbf{r}) = V_{WS}(\mathbf{r}) + V_{so}(\mathbf{r}) + V_C(\mathbf{r}), \quad (2)$$

where

$$V_{WS}(\mathbf{r}) = -V_0\{1 + \exp[(r - R(\theta,\varphi)/a)]\}^{-1}. \quad (3)$$

The depth of the WS potential for the protons and neutrons is set $V_0 = 54.25 \pm 39.6(N - Z)/A$ MeV. Here, we assume axially deformed nuclei with the nuclear surface defined as

$$R(\theta,\phi) = R_0\left[1 + \beta_0 + \sum_{\lambda=2,4} \beta_\lambda Y_{\lambda 0}(\theta,\varphi)\right], \quad (4)$$

where $R_0 = r_0 A^{1/3}$ is the radius of spherical nucleus with the radius parameter r_0, the value of β_0 takes into account the volume conservation, and β_2, β_4 are the parameters of quadrupole and hexadecapole deformations, respectively.

In Eq. (1), the term $H_{\rm pair}$ describes the pair correlations. The monopole pairing forces are used with the strength set to reproduce the odd-even difference of experimental nuclear masses. After Bogoliubov transformation, we obtain the Hamiltonian in terms of the quasiparticle creation and annihilation operators. The terms H_M and H_{SM} in Eq. (1) take into account the multipole and spin-multipole interactions between quasiparticles. To describe the long-range particle-hole residual interaction, we use the effective separable forces expressed through the operators of multipole and spin-multipole moments and write H_M and H_{SM} as

$$H_M = -\frac{1}{2}\sum_{l,\mu}\sum_{\tau,\rho=\pm1}\left(\kappa_0^{(l\mu)} + \rho\kappa_1^{(l\mu)}\right)M^+_{l\mu}(\tau)M_{l\mu}(\rho\tau),$$

$$H_{SM} = \sum_{l,\mu}\sum_{\lambda=l,l\pm1}\sum_{\tau,\rho=\pm1}\left(\kappa_0^{(l\lambda)} + \rho\kappa_1^{(l\lambda)}\right)M^{(\lambda)+}_{l\mu}(\tau)M^{(\lambda)}_{l\mu}(\rho\tau). \quad (5)$$

As seen, the H_M and H_{SM} generate phonon excitations in nuclei. Here, $\tau = N$ or Z. The isoscalar $\kappa_0^{(l\mu)}$ and isovector $\kappa_1^{(l\mu)}$ constants depend on angular momenta and their projection μ on the symmetry axis. The choice of their values was justified in Refs. [16,24,29]. The isoscalar constants are defined from the experimental phonon energies for even-even nuclei. The isovector constants are defined to describe the energy of isovector resonances. We have used the parameters suggested in Ref. [24] for the region of heavy nuclei. In accordance with Ref. [24], the ratio of isovector and isoscalar constants has been chosen as -1.5. Because the phonons with certain projection μ and parity π can be produced by forces with various angular momenta λ, the correct description requires elimination of spurious states with the same quantum numbers by using the phonon operator with certain μ and various multipolarities λ [25–27]. For example, the phonon with $\mu^\pi = 2^+$ contains electric-type components with $\lambda\mu = \{22,42,62,\dots\}$ and magnetic-type components with $L\lambda\mu = \{222,232,442,432,452,\dots\}$. The radial dependence of residual interaction is taken here as $\frac{d}{dr}V_{WS}(r)$. In this paper, we consider only the nonrotational states of nuclei. Therefore, the kinetic energy of rotation and the Coriolis interaction are not included in the Hamiltonian H.

After introduction of the phonon operators, the Hamiltonian (1) is rewritten in terms of the creation and annihilation operators for quasiparticles and phonons,

$$H = \sum_q \varepsilon_q \alpha_q^+\alpha_q + \sum_{\mu\pi i}\omega_{\mu^\pi i}Q^+_{\mu^\pi i}Q_{\mu^\pi i} + \sum_{qq'\mu\pi i}\Gamma_{qq'\mu\pi i}\alpha_q^+\alpha_{q'}(Q^+_{\mu^\pi i} + Q_{\mu^\pi i}), \quad (6)$$

where α_q^+ is the creation operator for quasiparticle in the state q with energy ε_q and $Q^+_{\mu^\pi i}$ is the creation operator for ith phonon of energy $\omega_{\mu^\pi i}$ in the state with certain μ and π. So, in the random phase approximation the problem is reduced to the determination of phonon energies in even-even nuclei and the excitation energies of A-odd nuclei obtained with allowance for the interaction of quasiparticles and phonons. Note that the amplitude $\Gamma_{qq'\mu\pi i}$ of the quasiparticle-phonon interaction does not contain free parameters and is uniquely determined by the matrix elements of the residual interaction, energy, and other phonon characteristics. The dependence on the phonon energy is of a pole nature that is decisive for calculating the spectra of A-odd nuclei. The Hamiltonian for an A-odd nucleus is diagonalized in the configuration space including one-quasiparticle states and quasiparticle $\otimes$ phonon states.

The wave function of an A-odd nucleus in the state with given K^π is as follows:

$$\Psi(K^\pi) = \left\{\sum_\rho C_\rho\alpha_\rho^+ + \sum_{\nu\mu\pi' i}D_{\nu\mu^{\pi' i}}\alpha_\nu^+Q^+_{\mu^{\pi' i}}\right\}\Psi_0 \quad (7)$$

with normalization

$$\sum_\rho (C_\rho)^2 + \sum_{\nu\mu\pi i}(D_{\nu\mu^\pi i})^2 = 1. \quad (8)$$

Here, Ψ_0 denotes the vacuum state for quasiparticles and phonons. The summation is over all single-particle states ρ, including the states with given K^π. The C_ρ and D_g are the amplitudes of the corresponding components of the wave function (7).

Solving the secular equation, we find the energy spectrum of the nucleus and the wave functions of its ground and excited states. In this paper we confine ourselves by the three lowest phonon states ($i = 1,2,3$) with $\mu = 0,1,2,3$. As shown, the contribution of higher multipolarities with $\lambda \geqslant 4$ and phonons with $i \geqslant 2$ to the states of A-odd nuclei with energies less than 1.2 MeV is small. The single-particle levels are taken into account from the bottom of the Woods-Saxon well to the energy of +5 MeV. Calculating the low-energy vibrational

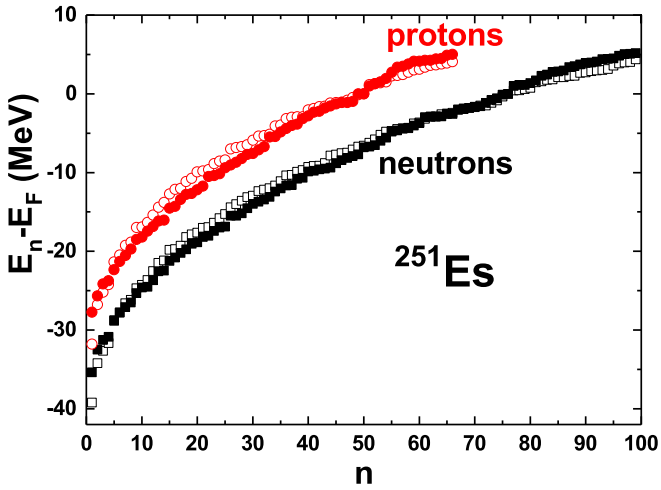

FIG. 1. Comparison of the calculated energies of single-particle levels in ^{251}Es for the Woods-Saxon potential (closed symbols) and the TCSM potential (open symbols). The results for protons and neutrons are shown by circles and squares, respectively. The energies are counted from the corresponding Fermi energies E_F.

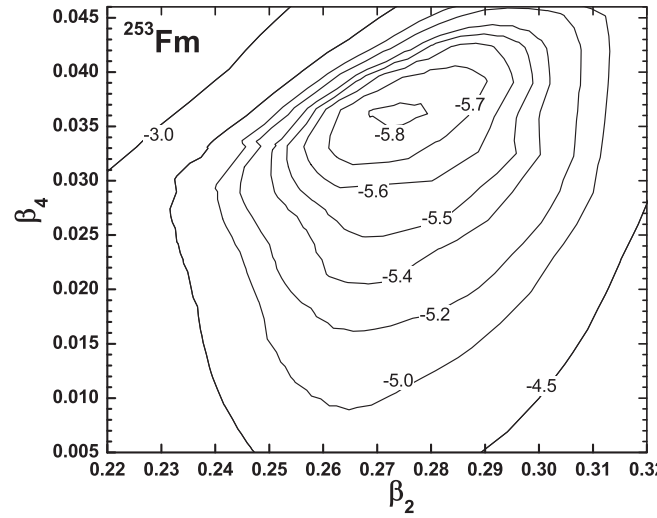

FIG. 2. Contour plot of the potential energy of ^{253}Fm as a function of β_2 and β_4. The energies are counted from the potential energy of spherical nucleus. The potential minimum is at $\beta_2 = 0.277$ and $\beta_4 = 0.037$.

states, we can also calculate the transitions between them. For example, in ^{248}Cm the calculated energies $E_{\lambda^\pi\mu}$ and corresponding transition probabilities $B(E\lambda;\lambda^\pi\mu \to 0^+0)$ ($E_{2^+0} = 1200$ keV, $B(E2;2^+0 \to 0^+0) = 1.62$ W.u.; $E_{2^+2} = 1300$ keV, $B(E2;2^+2 \to 0^+0) = 3.44$ W.u.; $E_{3^-0} = 1300$ keV, $B(E3;3^-0 \to 0^+0) = 6$ W.u.; $E_{3^-1} = 1000$ keV, $B(E3;3^-1 \to 0^+0) = 8.3$ W.u.; $E_{3^-2} = 900$ keV, $B(E3;3^-2 \to 0^+0) = 9$ W.u.; $E_{3^-3} = 1400$ keV, $B(E3;3^-3 \to 0^+0) = 5.1$ W.u.) are in a rather good agreement with available experimental data [57] ($E_{2^+2} = 1049$ keV, $B(E2;2^+2 \to 0^+0) = 3.89$ W.u.; $E_{3^-0} = 1094$ keV, $B(E3;3^-0 \to 0^+0) = 16$ W.u.; $E_{3^-3} = 1235$ keV, $B(E3;3^-3 \to 0^+0) = 5.87$ W.u.). So, our model can reproduce the low-energy vibrations with inaccuracy of 100–300 keV and transition probabilities within factor of 2–3 that is quite satisfactory.

III. CALCULATION OF GROUND-STATE DEFORMATIONS

The calculation of equilibrium deformations is carried out using the basis of the microscopic-macroscopic two-center shell model (TCSM) [47,50,51], taking into account the pairing and Strutinsky shell corrections [58,59]. Because the mean field of the Woods-Saxon form is used in the QPM [55], the single-particle states of the lower part of the TCSM spectrum for each deformation β_2 and β_4 are replaced by the corresponding states of the WS potential. With good accuracy, the energy spectra in these potentials almost coincide (Fig. 1) [56]. The single-particle energies E_n (n is the state number) for each spectrum are counted from the corresponding Fermi energies E_F of the proton and neutron systems. Note that the single-particle levels of the same energy in two potentials could have different asymptotic Nilsson numbers. However, the parameters can be adjusted to eliminate this problem at least for the levels near the Fermi surfaces. So, the similar results can be obtained with two different single-particle potentials.

The equilibrium deformation of the nucleus corresponds to the position of the minimum on the potential energy surface. To find it in the microscopic-macroscopic approach, one should minimize the deformation energy

$$E_{\rm def} = E_{LD} + E_{\rm sh} + E_{\rm pair} - E^0_{LD}, \qquad (9)$$

where E_{LD}, E_{sh}, and $E_{\rm pair}$ are the liquid-drop energy, the shell correction, and pairing correction, respectively. The deformation energy is counted from the liquid-drop energy E^0_{LD} of spherical nucleus.

In Figs. 2–4, the contour plots of $E_{def}(\beta_2,\beta_4)$ near the ground states are shown for ^{253}Fm, ^{251}No, and ^{286}Fl. The

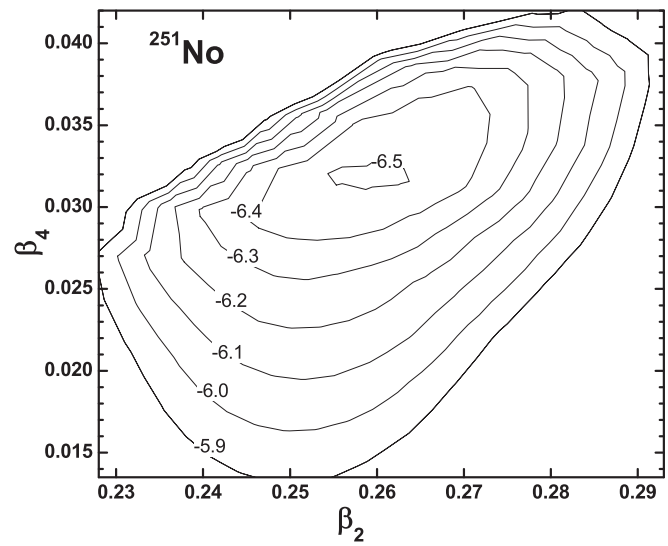

FIG. 3. Contour plot of the potential energy of ^{251}No as a function of β_2 and β_4. The energies are counted from the potential energy of spherical nucleus. The potential minimum is at $\beta_2 = 0.266$ and $\beta_4 = 0.033$.

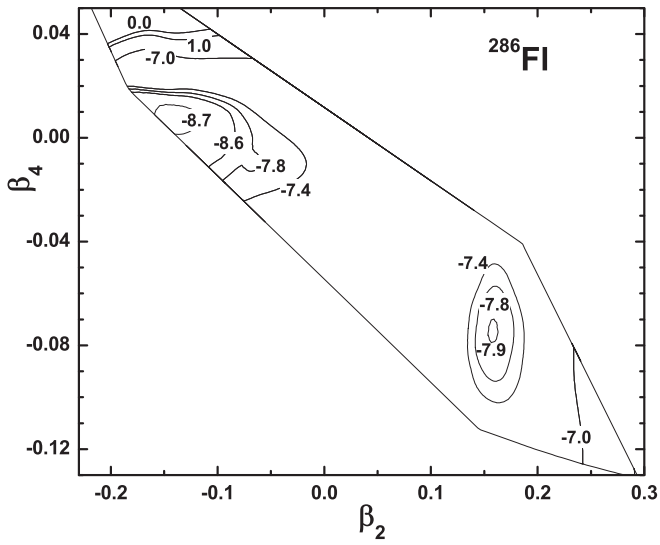

FIG. 4. Contour plot of the potential energy of ^{286}Fl as a function of β_2 and β_4. The energies are counted from the potential energy of spherical nucleus. There are two potential minimum at $\beta_2 = -0.136$, $\beta_4 = 0.009$ and $\beta_2 = 0.161$, $\beta_4 = -0.074$.

relationship between the coordinate of the TCSM and parameters β_2 and β_4 in Eq. (4) is established from the equality of the corresponding calculated multipole moments. Figures 2–4 clearly show the ground-state potential minimum corresponding to the equilibrium deformations of these nuclei. In some cases, there exist less pronounced additional local potential minima that can be interpreted as possible shape isomeric states of the nuclei. For example, in Fig. 4 for ^{286}Fl there are two minima which differ in energy by approximately 0.9 MeV and have opposite signs of deformations. The nuclear shapes in these two potential minima are presented in Fig. 5.

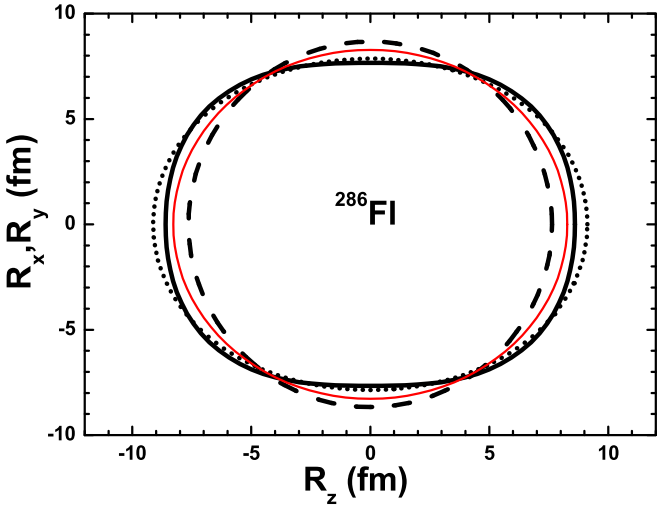

FIG. 5. Nuclear shapes $R(\theta)$ of ^{286}Fl in two potential minima shown in Fig. 4. The nuclear shapes for positive and negative values of β_2 are shown by solid and dashed lines, respectively. The nuclear shape shown by solid line is transformed into that shown by dotted line at $\beta_4 = 0$. The shape of spherical nucleus is shown by thin red line.

TABLE I. Calculated equilibrium deformations of nuclei indicated.

Nucleus	β_2	β_4	Nucleus	β_2	β_4
^{243}Cm	0.272	0.041	^{251}No	0.261	0.037
^{245}Cm	0.272	0.041	^{253}No	0.263	0.035
^{247}Cm	0.275	0.039	^{255}No	0.257	0.027
^{249}Cm	0.272	0.041	^{257}No	0.253	0.016
^{251}Cm	0.272	0.041	^{259}No	0.256	0.002
^{245}Cf	0.275	0.039	^{255}Rf	0.253	0.002
^{247}Cf	0.275	0.039	^{257}Rf	0.262	0.023
^{249}Cf	0.275	0.039	^{259}Rf	0.251	−0.010
^{251}Cf	0.279	0.035	^{261}Rf	0.246	0.020
^{253}Cf	0.266	0.033	^{259}Sg	0.262	−0.006
^{255}Cf	0.279	0.035	^{261}Sg	0.266	−0.008
^{249}Fm	0.275	0.039	^{263}Sg	0.259	−0.031
^{251}Fm	0.279	0.035	^{265}Sg	0.262	−0.037
^{253}Fm	0.277	0.037	^{263}Hs	0.263	−0.034
^{255}Fm	0.277	0.037	^{265}Hs	0.246	0.049
^{257}Fm	0.273	0.013	^{267}Hs	0.269	−0.054
^{259}Fm	0.247	0.007	^{269}Hs	0.254	−0.055

The ground-state equilibrium deformations calculated for indicated N-odd heavy nuclei with $96 \leqslant Z \leqslant 108$ are listed in Table I. The single-particle spectra of the WS potential are used to calculate E_{def}. As found, the single-particle spectra of the TCSM potentials result in close values of deformation parameters at the ground state. For β_2, the difference does not exceed 10%.

IV. DEPENDENCE OF CALCULATED RESULTS ON THE QPM PARAMETERS

Based on the large number of calculations of one-quasiparticle spectra of heavy nuclei, the "basic" set of the WS parameters and spin-orbit strength were suggested in Table II. These parameters together with the quasiparticle-phonon strength were adjusted to have a good description of the spectra and transitions in them for well-studied heavy nuclei. The depth of the spin-orbit potential is assumed to be equal to the depth of the mean field. In Ref. [24], the parameters of the WS potential were suggested for each region of nuclide map. Here, we use one parameter set for heavy and superheavy nuclei. The parameters of pairing interaction are from the difference of the mass of neighboring nuclei (experimental, if known, or extrapolated). In Fig. 6, for ^{249}Cm the calculated energies of the lowest nonrotational states are presented and compared with the experimental values. The calculations are performed with the basic set of the WS parameters as well as with other sets to demonstrate the sensitivity of the results to

TABLE II. Basic parameters of the WS potential and spin-orbit strengths κ adjusted for neutrons and protons of heavy nuclei.

	r_0 (fm)	a (fm)	κ (fm)^2
Neutrons	1.26	0.80	0.450
Protons	1.24	0.65	0.320

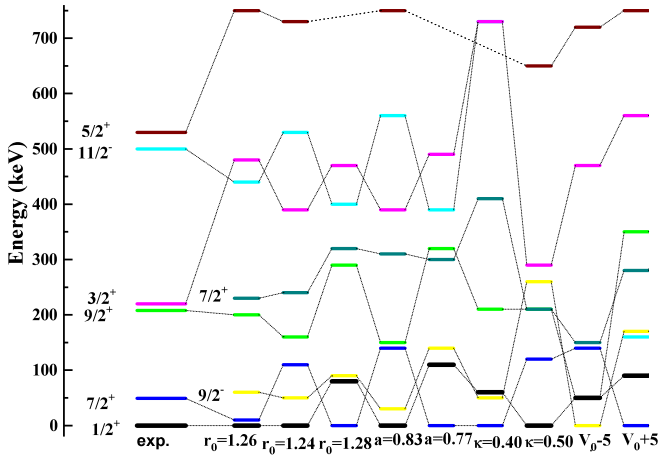

FIG. 6. The spectra of low-lying nonrotational states in ^{249}Cm. The calculated results are obtained with various parameters of the WS potential and compared with the experimental data (exp) [57]. The second column presents the results obtained with the parameters from Table II. In other columns, the results are obtained with indicated parameter for neutrons different from those given in Table II. The depth of the WS potential is taken to be $V_0 = 54.25 \pm 39.6\,(N-Z)/A$.

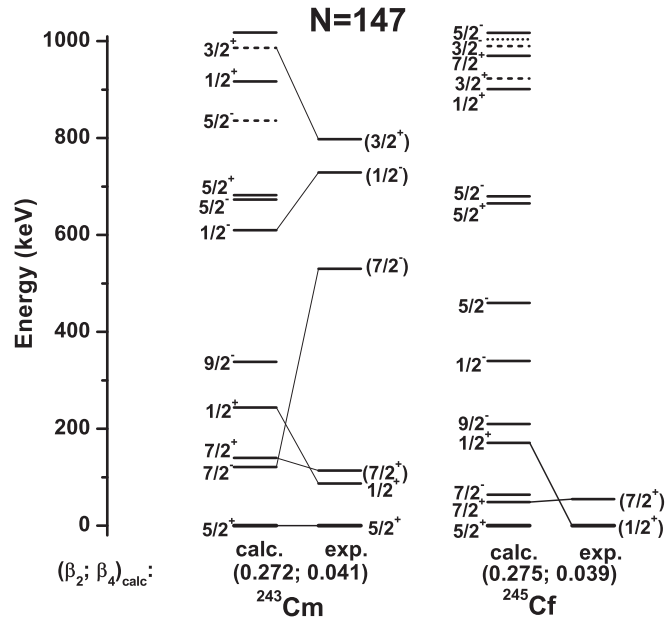

FIG. 7. Calculated spectra of low-lying states are compared with the available experimental data [57] for $N = 147$ isotones. The solid lines denote the states with one-quasiparticle component contributing more than 70% of the norm. The dotted lines correspond to the states with the quasiparticle ⊗ phonon component exceeding 70%. Other states are denoted by the dashed lines. The value of K in brackets means the tentative assignment.

the variation of the WS parameters. As seen, the reasonable variations of radius parameter and diffuseness do not cause large changes in the energy spectrum. The largest changes are caused by the variation of the spin-orbit strength. However, even in this case the deviation of the calculated energies from the experimental ones does not exceed 300 keV, which is still acceptable. So, 10% deviation from the parameters presented in Table II does not destroy a rather good agreement with the experimental data.

The basic set of parameters of the Woods-Saxon potential, presented in Table II, is used further in the present work for calculating the spectra of nonrotational states. The multipole interaction constants are established for phonons with $\mu \leqslant 3$. The results obtained with inclusion of $3 < \mu \leqslant 7$ change very little in comparison to those obtained with $\mu \leqslant 3$. The calculated phonon energies are seemed to be close to the known experimental values for the even-even core. If we would vary these energies to see the sensitivity of the calculated spectra, the energies of the levels with relatively large admixture of phonon component change. However, these levels are usually located at energies larger than 400 keV. These levels are also the most sensitive to the variation of the multipole constants. So, the quasiparticle-phonon interaction can crucially influence the nonrotational state if its energy is larger than 400 keV.

V. NONROTATIONAL STATES IN ISOTONIC CHAINS

Using the basic parameters of the WS potential (Table II) [15,16], we calculate the ground-state values of β_2 and β_4 (Table I) with the microscopic-macroscopic approach described. The single-particle spectra lying near the Fermi surface are used to calculate the nonrotational spectra and their quasiparticle-phonon structures with the QPM. The isotones with $N = 147$, 149, 151, 153, 155, 157, 159, and 161 are considered to trace the dependence of low-lying nonrotational states on Z.

The comparison of the calculated energy spectra with the available experimental data [57] is shown in Fig. 7 for two $N = 147$ isotones. The calculated structures of low-lying nonrotational states are presented in the Supplemental Material [60]. In most cases, the model satisfactory describes the data taking their uncertainties into account. A rather good agreement with the experimental data is seen in Figs. 8

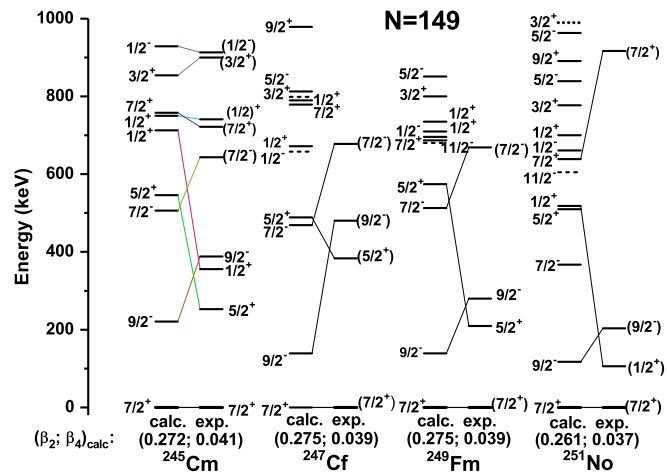

FIG. 8. The same as in Fig. 7, but for the $N = 149$ isotones.

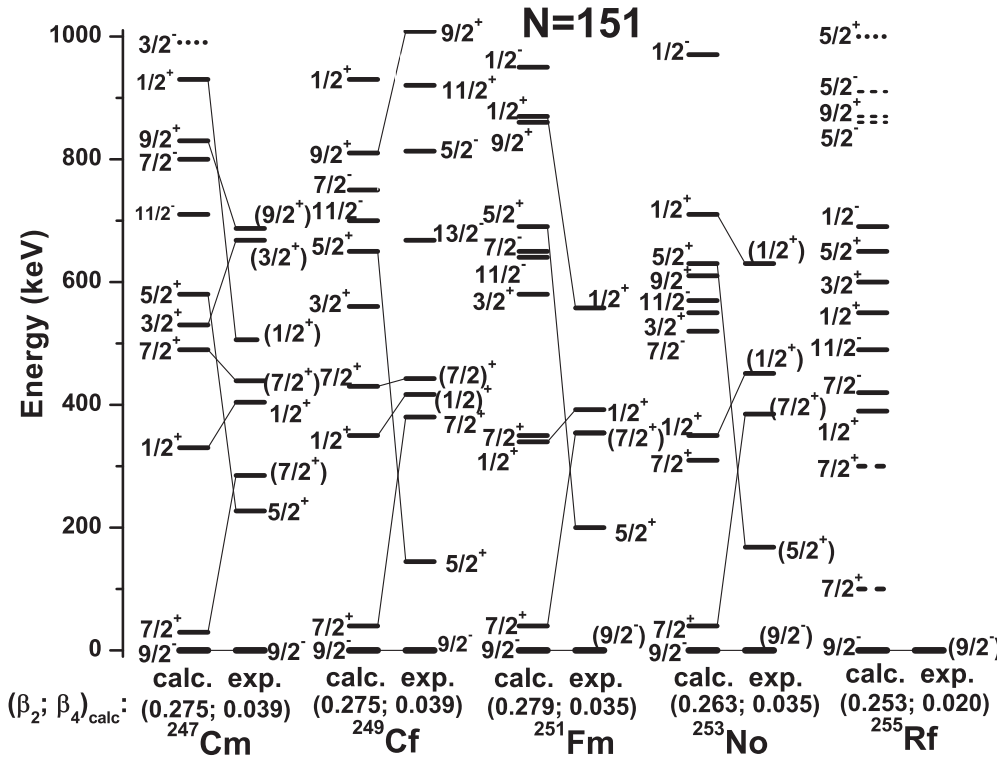

FIG. 9. The same as in Fig. 7, but for the $N = 151$ isotones.

and 9, presenting the calculated spectra for $N = 149$ and 151 isotones. The ground-state characteristics are correctly reproduced. As in Ref. [50], the energies of the level with the same Nilsson quantum numbers smoothly change with Z if the the deformations of isotones are close to each other. In Fig. 9, the inversion of $1/2^+$ and $5/2^+$ levels in the experimental

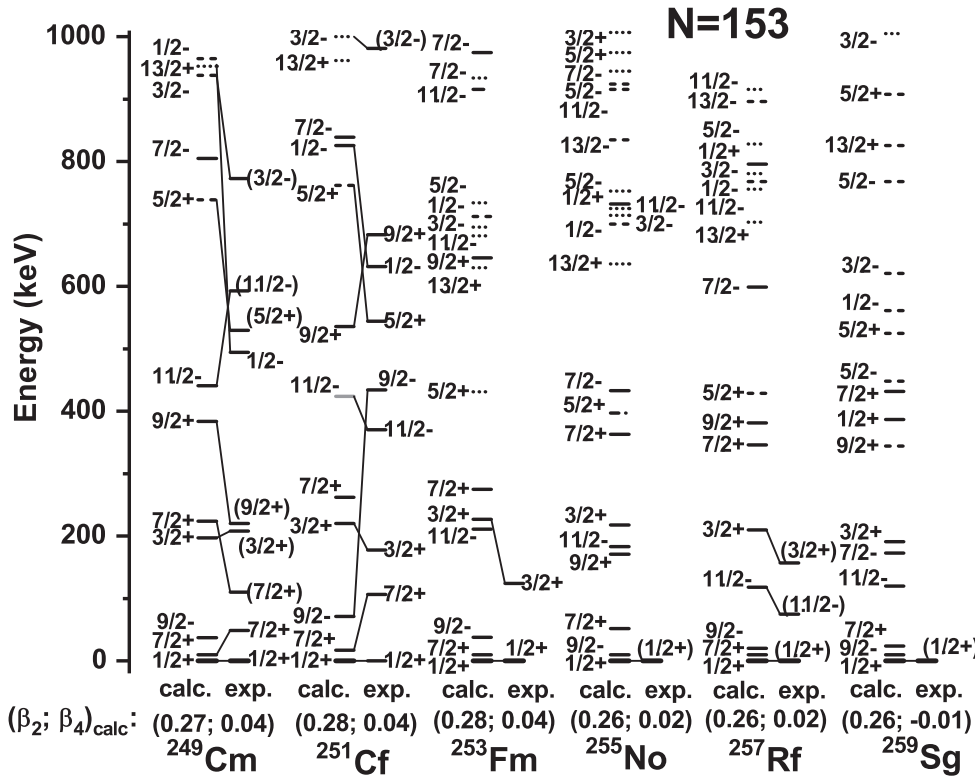

FIG. 10. The same as in Fig. 7, but for the $N = 153$ isotones.

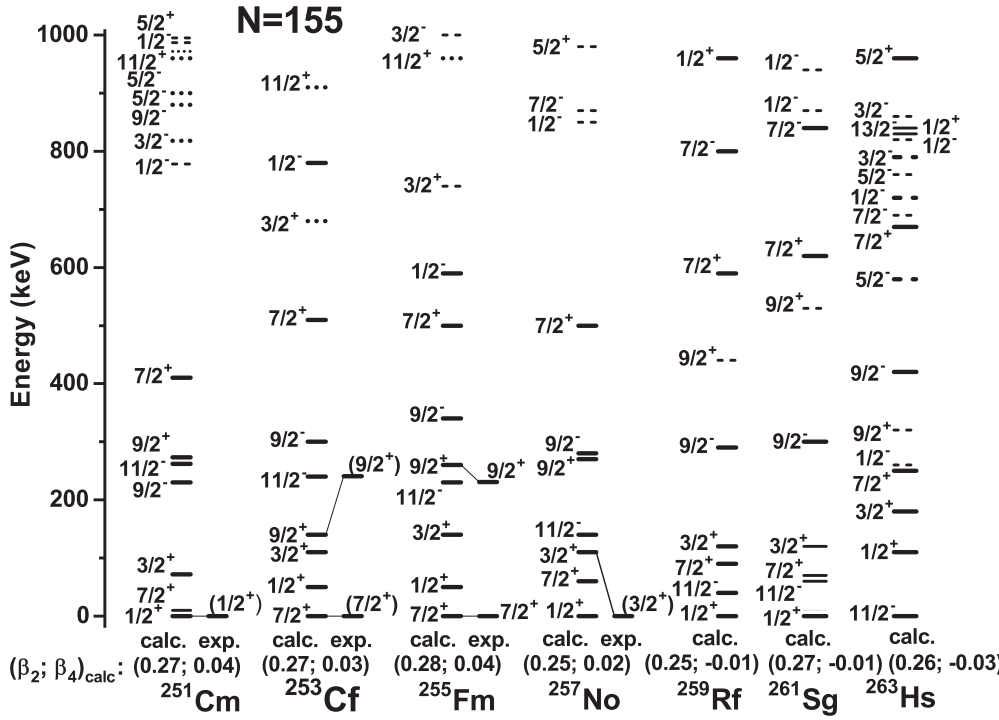

FIG. 11. The same as in Fig. 7, but for the $N = 155$ isotones.

spectra compared to the calculated ones reduces the lifetime of $1/2^+$ state. However, it still about 100 ns [57].

In $N = 153$ isotones (Fig. 10), the spectra are quite dense near the ground states. So, the small change of the ground-state deformation could change the order of levels. Except for a few cases, the experimental levels are well described. The sequence of calculated states almost corresponds to that in the experimental spectrum. Two first states $1/2^+$ and $7/2^+$ are close in energy. So, the low-lying isomeric state is expected in $N = 153$ isotones.

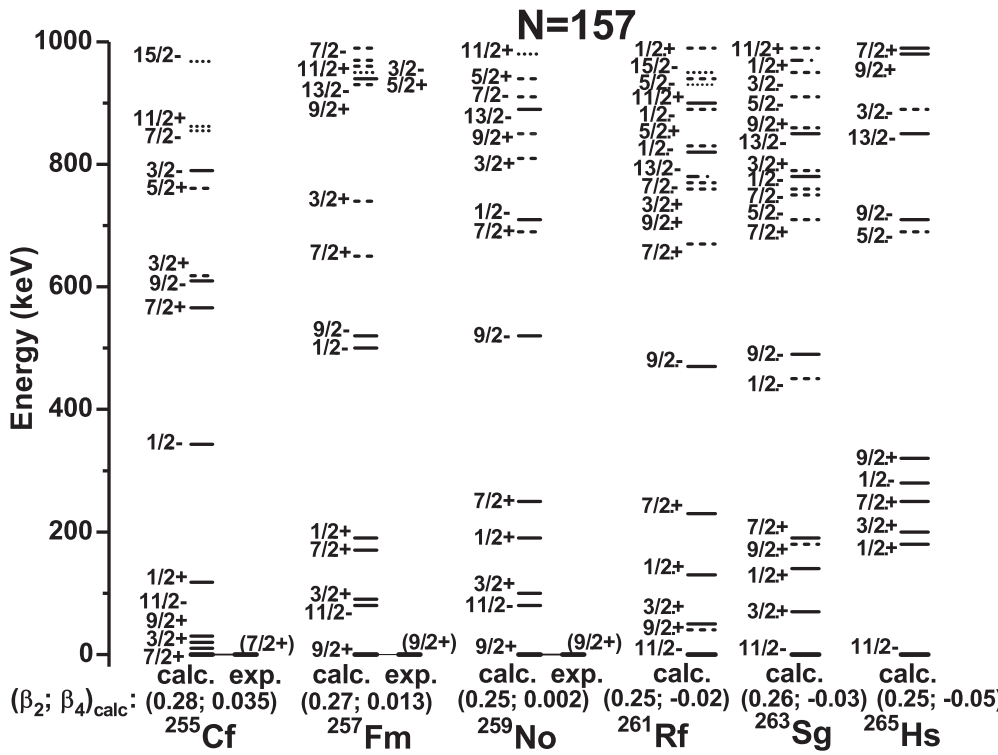

FIG. 12. The same as in Fig. 7, but for the $N = 157$ isotones.

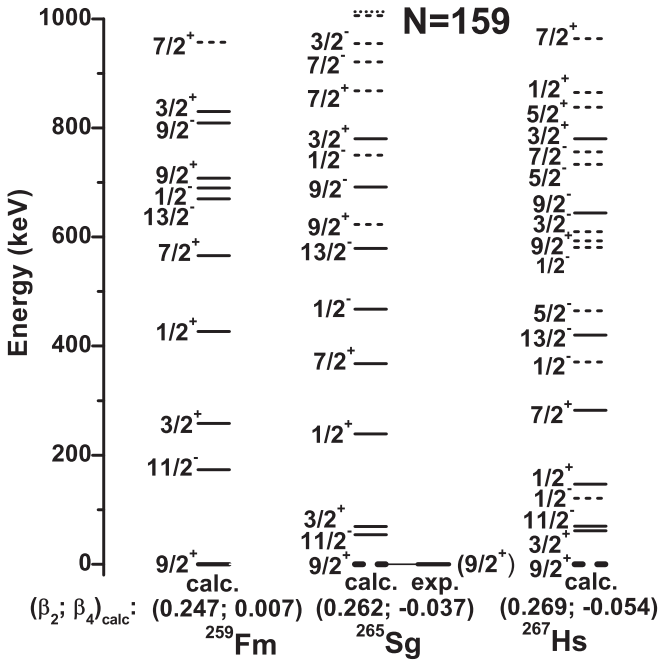

FIG. 13. The same as in Fig. 7, but for the $N = 159$ isotones.

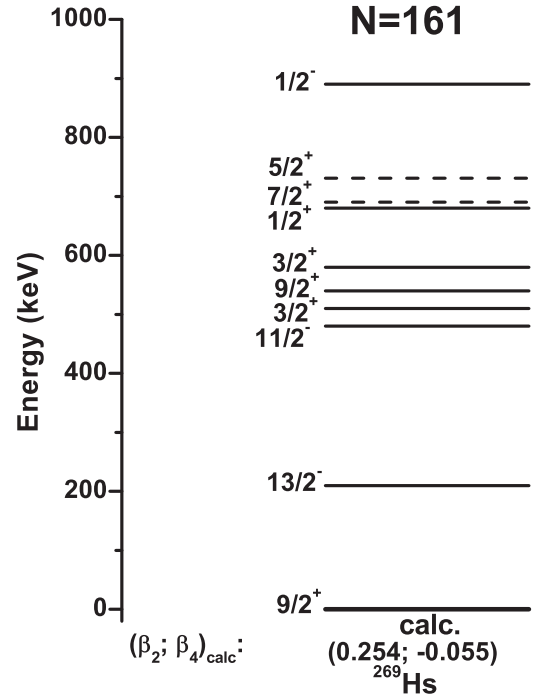

FIG. 14. The same as in Fig. 7, but for ^{269}Hs as an example of nucleus with $N = 161$.

The lowest calculated states in the $N = 155$ isotonic chain (Fig. 11) have $\Delta K \geqslant 3$. Therefore, the long-living isomeric state is expected in $N = 155$ isotones. If the energy of this isomer is small, its lifetime is long enough and the α decay could occur from this isomer. As seen, the calculated ground-sate spin changes in ^{257}No when the value of β_4 decreases. Therefore, the small change of the deformation could cause the inversion of the levels $1/2^+$ and $7/2^+$, which are close in energy, in the dense spectrum.

In the $N = 157$ isotonic chain (Fig. 12), the ground-state hexadecapole deformation decreases with increasing Z. This changes the ground-state spin and the order of low-lying levels. The lowest calculated states in ^{263}Sg and ^{265}Hs (Fig. 11) have $\Delta K \geqslant 4$. So, the first excited states in ^{263}Sg and ^{265}Hs can be related to the observed isomeric states [57] at 130 and above 300 keV, respectively. The lowest $3/2^+$ state could be isomeric in ^{257}Fm, ^{259}No, and ^{261}Rf. In the latter nucleus, the isomeric state has been found at 234 keV [57].

Because of the change in the ground-state deformation, the spectrum becomes denser with Z in the $N = 159$ isotonic chain (Fig. 13). As in Fig. 12, the lowest $3/2^+$ state could be the isomeric one. Indeed, there are experimental indications [57] for the existence of low-lying isomeric states in the $N = 159$ isotones.

To find the nuclear binding energy, we still have to adjust the parameters of macroscopic and maybe microscopic parts of the potential energy. In Ref. [51], we presented such type of calculations, but for the two-center oscillator potential. We would like to leave the calculations of the binding energies with the Woods-Saxon mean-field for future work. Because the single-particle wave functions are calculated, the mass and charge radii can be found as well. There are more experimental data on α decays. The values of Q_α are defined by the difference of corresponding binding energies and, thus, are less sensitive to the uncertainties of the present calculation. For nuclei ^{267}Hs, ^{263}Sg, ^{259}Sg, and ^{255}No of α-decay chain of ^{267}Hs, the calculated preliminary Q_α are 9.61, 9.3, 9, and 8.47 MeV, respectively, which are in a good agreement with the experimental values [57] 9.98, 9.4, 9.13, and 8.43 MeV, respectively. One can find more examples in Ref. [52].

As an example of $N = 161$ nucleus, the calculated spectrum of ^{269}Hs is shown in Fig. 14. One can see that the low-lying isomeric states are not expected in the $N = 161$ isotonic chain.

Let us consider the ground-states spins of isotones. For $N = 149$ and 151 isotones, the ground-state values of K^π are $7/2^+$ and $9/2^-$, respectively. The ground-state spin can change in the isotone chain if the deformation varies due to the cross of proton shell or subshell. The residual interaction and phonon coupling could also change the order of the quasiparticle levels in the case of the dense single-particle spectrum. For example, in the isotone chain with $N = 153$ the sequence of the close quasiparticle states $7/2^+[613]$ and $1/2^+[620]$ changes due to even small change of the ground-state deformation. In the $N = 155$ isotones, the quasiparticle-phonon interaction lowers the $7/2^+$ state with respect to the closest $1/2^+[620]$ state. This corresponds to the experimental data. Table III summarizes the results of our description of the ground-state spins. In most cases, our results correspond to the experimental assignments [57]. In ^{245}Cf and ^{257}No, the calculated ground-state spins deviate from the experimental assignments. In these nuclei, the level with the experimental value of spin is close in energy to the calculated ground-state level, within 200- to 300-keV inaccuracy of the QPM.

The results of our calculations demonstrate a rather good description of many low-lying states. However, the energies of

TABLE III. Calculated and experimental ground-state spins of the indicated nuclei with $N = 147$–161. The tentative assignments of the spins are in the brackets.

N	Cm		Cf		Fm		No		Rf		Sg		Hs
	Exp.	Calc.	Exp.	Calc.	Exp.	Calc.	Exp.	Calc.	Exp.	Calc.	Exp.	Calc.	Calc.
147	$5/2^+$	$5/2^+$	$(1/2^+)$	$5/2^+$									
149	$7/2^+$	$7/2^+$	$(7/2^+)$	$7/2^+$	$(7/2^+)$	$7/2^+$	$(7/2^+)$	$7/2^+$					
151	$9/2^-$	$9/2^-$	$9/2^-$	$9/2^-$	$(9/2^-)$	$9/2^-$	$(9/2^-)$	$9/2^-$	$(9/2^-)$	$9/2^-$			
153	$1/2^+$	$1/2^+$	$1/2^+$	$1/2^+$	$1/2^+$	$1/2^+$	$(1/2^+)$	$1/2^+$	$(1/2^+)$	$1/2^+$	$(1/2^+)$	$1/2^+$	
155	$(1/2^+)$	$1/2^+$	$(7/2^+)$	$7/2^+$	$7/2^+$	$7/2^+$	$(3/2^+)$	$1/2^+$		$1/2^+$		$1/2^+$	$11/2^-$
157			$(7/2^+)$	$7/2^+$	$(9/2^+)$	$9/2^+$	$(9/2^+)$	$9/2^+$		$11/2^-$		$11/2^-$	$11/2^-$
159						$9/2^+$					$(9/2^+)$	$9/2^+$	$9/2^+$
161													$9/2^+$

some states are underestimated. In $N = 151$ isotones, we get two low-lying $7/2^+$ states. As seen in Table IV, the lowest one $7/2^+[624]$ has the energy 30–100 keV, but in the experiment it is at 285–385 keV. Similar disagreement is also seen in other theoretical calculations mentioned in Table IV. If one level is better described in some approach, one can usually find another level whose description is worse. In $N = 153$ isotones, we underestimate the energy of the $9/2^-[734]$ state in comparison to the experiment. However, for nuclei beyond Cf only a few levels are firmly defined in the experiment.

VI. SUMMARY

The systematic calculations of low-lying states were performed in the $N = 147$–161 isotones of heavy nuclei. The QPM was used to take into account the residual paring and phonon-quasiparticle interactions. This model was improved by finding out the ground-state deformations for each nucleus using the microscopic-macroscopic approach. As shown, the effects beyond the mean-field influence the order of the levels in quite dense spectra. The phonon-quasiparticle interaction is mainly important for the states above 400 keV. The energies of the low-lying states are reproduced within 300 keV, which seems to be a quite good description. Note that the calculations for all isotonic chains were performed with the fixed parameters of the Hamiltonian, which seem to be reliable in the wide region of nuclear chart. If the lowest excited state differs by $\Delta K \geqslant 3$ with the ground state, one can expect an appearance of the isomeric state. In heaviest nuclei, the α decay from these isomeric states could occur. The estimate of isomer lifetime is

TABLE IV. Comparison of calculated (th.) nonrotational spectra in $N = 151$ isotones with other calculations and the available experimental data. The tentatively assigned energies are in the brackets.

Nucleus	$633\downarrow$	$501\downarrow$	$631\downarrow$	$743\uparrow$	$622\uparrow$	$624\downarrow$	$734\uparrow$	$613\uparrow$	$620\uparrow$	$622\downarrow$	$725\uparrow$	$615\downarrow$	$752\downarrow$
^{247}Cm [61,62]			(506)		227	(285)	0	(<439)	405	(668)		(<687)	
th.	1020		930	800	580	30	0	490	330	530	710	830	990
[11]			800	790	380	170	0	640	540	680	920		
[8]			590		530	220	0	650		760	1040		
[29]	1096	1327	859	818	647	84	0	218	467	677	691	811	1052
[21]		800	570	730	480	50	0	240	210	350	450	1050	870
^{249}Cf [63]				(1218)	145	380	0	(443)	(417)			1008	
th.	1060		930	750	650	40	0	430	350	560	700	810	
[11]			800	810	360	170	0	720	590	720	920		
[8]			980		490	220	0	790	620	780	1050		
[29]	980		850	820	610	50	0	210	450	650	620	800	890
^{251}Fm [64]			392		200	(354)	(0)		558				
th.		950	870	650	690	40	0	340	340	580	640	860	
[11]		900	780	810	330	180	0	880	630	760	950		
[8]					440	890	0	210	650	790	1030		
[29]	1080		830	800	600	50	0	200	450	530	650	790	1050
^{253}No [64,65]			(630)		167	(385)	(0)		450				
th.	1040	970	710	520	630	40	0	310	350	550	570	610	
[11]		690	700	780	320	200	0		660	730			
[8]					410	950	0	240	670	800	1000	1500	
[29]	1100		800	770	600	200	0	50	400	650	660	700	1050
^{255}Rf [64]							(0)						
th.	1000	690	550	420	650	100	0	300	390	600	490	870	1100
[11]		580	630	750	320	250	0	920	650	750	820		
[8]					400	920	0	290	670	790	890		

a separate complicated problem. As is known, the simple Weisskopf estimates strongly overestimate the isomer lifetimes. To be more precise, one should to take into account the Corriolis and other effects which influence the width of isomeric state. Comparing our calculated results with those obtained earlier without taking the phonon-quasiparticle interaction into account, one can conclude that some improvement of the excitation spectra is achieved in the calculations presented. One way to improve further the description of the experimental data and increase the predictive power of the model is the extraction of the single-particle potential for the QPM from the self-consistent approaches. In this case, one can combine the advantages of the QPM with the self-consistent microscopic methods.

ACKNOWLEDGMENTS

This work was supported by the RFBR (Russia) and DFG (Bonn). The Polish-JINR (Dubna) Cooperation Programm is gratefully acknowledged. N.V.A. was supported by Tomsk Polytechnic University Competitiveness Enhancement Program grant.

[1] Yu. Ts. Oganessian, J. Phys. G **34**, R165 (2007).
[2] Y. T. Oganessian, F. S. Abdullin, P. D. Bailey, D. E. Benker, M. E. Bennett, S. N. Dmitriev, J. G. Ezold, J. H. Hamilton, R. A. Henderson, M. G. Itkis *et al.*, Phys. Rev. Lett. **104**, 142502 (2010).
[3] Y. T. Oganessian, F. S. Abdullin, S. N. Dmitriev, J. M. Gostic, J. H. Hamilton, R. A. Henderson, M. G. Itkis, K. J. Moody, A. N. Polyakov, A. V. Ramayya *et al.*, Phys. Rev. C **87**, 014302 (2013).
[4] S. Hofmann, D. Ackermann, S. Antalic, H. G. Burkhard, V. F. Comas, R. Dressler, Z. Gan, S. Heinz, J. A. Heredia, F. P. Heßberger *et al.*, Eur. Phys. J. A **32**, 251 (2007).
[5] R.-D. Herzberg and P. T. Greenlees, Prog. Part. Nucl. Phys. **61**, 674 (2008).
[6] F. P. Heßberger, Eur. Phys. J. D **45**, 33 (2007).
[7] B. Streicher *et al.*, Eur. Phys. J. A **45**, 275 (2010).
[8] S. Ćwiok, S. Hofmann, and W. Nazarewicz, Nucl. Phys. A **573**, 356 (1994).
[9] S. Ćwiok, W. Nazarewicz, and P. H. Heenen, Phys. Rev. Lett. **83**, 1108 (1999).
[10] A. Parkhomenko and A. Sobiczewski, Acta Phys. Pol. B **35**, 2447 (2004).
[11] A. Parkhomenko and A. Sobiczewski, Acta Phys. Pol. B **36**, 3115 (2005).
[12] E. Litvinova, Phys. Rev. C **85**, 021303(R) (2012).
[13] A. V. Afanasjev and E. Litvinova, Phys. Rev. C **92**, 044317 (2015).
[14] E. Litvinova, Phys. Rev. C **91**, 034332 (2015).
[15] V. G. Soloviev, *Theory of Complex Nuclei* (Pergamon Press, Oxford, UK, 1976).
[16] V. G. Soloviev, *Theory of Atomic Nuclei: Quasiparticles and Phonons* (Institute of Physics Publishing, Bristol, 1992).
[17] N. Lo Iudice and Ch. Stoyanov, Phys. Rev. C **65**, 064304 (2002).
[18] N. Tsoneva, Ch. Stoyanov, Yu. P. Gangrsky, V. Yu. Ponomarev, N. P. Balabanov, and A. P. Tonchev, Phys. Rev. C **61**, 044303 (2000).
[19] N. Van Giai, Ch. Stoyanov, V. V. Voronov, and S. Fortier, Phys. Rev. C **53**, 730 (1996).
[20] A. L. Komov, L. A. Malov, and V. G. Soloviev, Izv. AN SSSR, Ser. Fiz. **35**, 1550 (1971).
[21] F. A. Gareev, S. P. Ivanova, L. A. Malov, and V. G. Soloviev, Nucl. Phys. A **171**, 134 (1971).
[22] S. P. Ivanova, A. L. Komov, L. A. Malov, and V. G. Soloviev, Izv. AN SSSR, Ser. Fiz. **39**, 1612 (1975).
[23] S. P. Ivanova, A. L. Komov, L. A. Malov, and V. G. Soloviev, Izv. AN SSSR, Ser. Fiz. **37**, 911 (1973).
[24] L. A. Malov and V. G. Soloviev, Phys. Part. Nuclei **11**, 111 (1980).
[25] R. Nojarov and A. Faessler, Nucl. Phys. A **484**, 1 (1988).
[26] V. G. Soloviev, A. V. Sushkov, and N. Yu. Shirikova, Phys. Part. Nuclei **25**, 157 (1994).
[27] L. A. Malov, Izv. RAN, Ser. Fiz. **60**, 47 (1996).
[28] N. Yu. Shirikova, A. V. Sushkov, and R. V. Jolos, Phys. Rev. C **88**, 064319 (2013).
[29] N. Yu. Shirikova, A. V. Sushkov, L. A. Malov, and R. V. Jolos, Eur. Phys. J. A **51**, 21 (2015).
[30] P. Möller, J. R. Nix, W. D. Myers, and W. J. Swiatecki, At. Data Nucl. Data Table **59**, 185 (1995).
[31] K. E. G. Lobner, M. Vetter, and V. Honig, Nucl. Data Table **A7**, 495 (1970).
[32] J. Meng, H. Toki, S. G. Zhou, S. Q. Zhang, W. H. Long, and L. S. Geng, Prog. Part. Nucl. Phys. **57**, 470 (2006).
[33] S.-H. Shen, J.-N. Hu, H.-Z. Liang, J. Meng, P. Ring, and S. Q. Zhang, Chin. Phys. Lett. **33**, 102103 (2016).
[34] S. Shen, H. Liang, J. Meng, P. Ring, and S. Zhang, Phys. Rev. C **96**, 014316 (2017).
[35] S.-G. Zhou, J. Meng, and P. Ring, Phys. Rev. C **68**, 034323 (2003).
[36] J. Meng, K. Sugawara-Tanabe, S. Yamaji, and A. Arima, Phys. Rev. C **59**, 154 (1999).
[37] S.-G. Zhou J. Meng, and P. Ring, Phys. Rev. Lett. **91**, 262501 (2003).
[38] Z.-Y. Ma, J. Rong, B.-Q. Chen, Z.-Y. Zhu, and H.-Q. Song, Phys. Lett. B **604**, 170 (2004).
[39] W.-H. Long, N. Van Giai, and J. Meng, Phys. Lett. B **640**, 150 (2006).
[40] G. A. Lalazissis, J. Konig, and P. Ring, Phys. Rev. C **55**, 540 (1997).
[41] A. T. Kruppa, M. Bender, W. Nazarewicz, P.-G. Reinhard, T. Vertse, and S. Cwiok, Phys. Rev. C **61**, 034313 (2000).
[42] Y. Shi, D. E. Ward, B. G. Carlsson, J. Dobaczewski, W. Nazarewicz, I. Ragnarsson, and D. Rudolph, Phys. Rev. C **90**, 014308 (2014).
[43] S.-G. Zhou, Phys. Scr. **91**, 063008 (2016).
[44] Z.-X. Li, Z.-H. Zhang, and P.-W. Zhao, Front. Phys. **10**, 102101 (2015).
[45] M. Bender, P.-H. Heenen, and P.-G. Reinhard, Rev. Mod. Phys. **75**, 121 (2003).

[46] P. Klupfel, P.-G. Reinhard, T. J. Burvenich, and J. A. Maruhn, Phys. Rev. C **79**, 034310 (2009).
[47] J. Maruhn and W. Greiner, Z. Physik **251**, 431 (1972).
[48] G. G. Adamian, N. V. Antonenko, and W. Scheid, Phys. Rev. C **81**, 024320 (2010).
[49] G. G. Adamian, N. V. Antonenko, S. N. Kuklin, and W. Scheid, Phys. Rev. C **82**, 054304 (2010).
[50] G. G. Adamian, N. V. Antonenko, S. N. Kuklin, B. N. Lu, L. A. Malov, and S. G. Zhou, Phys. Rev. C **84**, 024324 (2011).
[51] A. N. Kuzmina, G. G. Adamian, N. V. Antonenko, and W. Scheid, Phys. Rev. C **85**, 014319 (2012).
[52] V. G. Kartavenko, N. V. Antonenko, A. N. Bezbakh, L. A. Malov, N. Yu. Shirikova, A. V. Sushkov, and R. V. Jolos, Chin. Phys. C **41**, 074105 (2017).
[53] S. P. Ivanova, A. L. Komov, L. A. Malov, and V. G. Soloviev, Phys. Part. Nucl. **7**, 450 (1976).
[54] V. G. Soloviev, A. V. Sushkov, and N. Yu. Shirikova, Phys. Part. Nucl. **27**, 667 (1996).
[55] F. A. Gareev, S. P. Ivanova, and B. N. Kalinkin, Izv. AN SSSR, Ser. Fiz. **33**, 1690 (1968).
[56] N. V. Antonenko and L. A. Malov, Bull. Rus. Acad. Sc., Physics **78**, 1137 (2014).
[57] http://www.nndc.bnl.gov/nndc/ensdf/.
[58] V. M. Strutinsky, Sov. J. Nucl. Phys. **3**, 149 (1966).
[59] V. M. Strutinsky, Nucl. Phys. A **95**, 420 (1976).
[60] See Supplemental Material at http://link.aps.org/supplemental/10.1103/PhysRevC.97.034308 for more information about the calculated structures of low-lying nonrotational states.
[61] T. H. Braid, R. R. Chasman, J. R. Erskine, and A. M. Fridman, Phys. Rev. C **4**, 247 (1971).
[62] C. D. Nesaraja, Nucl. Data Sheets **125**, 395 (2015).
[63] K. Abusaleem, Nucl. Data Sheets **112**, 2129 (2011).
[64] E. Brown and J. K. Tuli, Nucl. Data Sheets **114**, 1041 (2013).
[65] A. Artna-Cohen, Nucl. Data Sheets **88**, 155 (1999).